

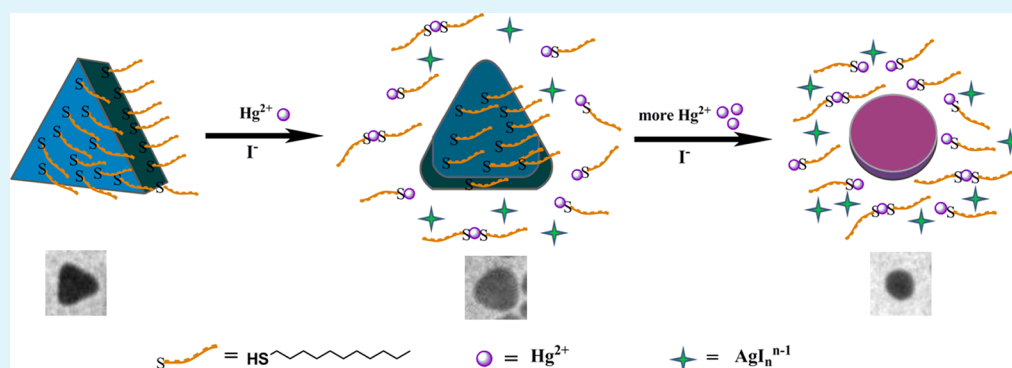
Highly Sensitive and Selective Colorimetric Sensing of Hg^{2+} Based on the Morphology Transition of Silver Nanoprisms

Ling Chen,^{†,‡} Xiuli Fu,^{†,‡} Wenhui Lu,[†] and Lingxin Chen^{*,†}

[†]Key Laboratory of Coastal Zone Environmental Processes, Yantai Institute of Coastal Zone Research, Chinese Academy of Sciences, Yantai 264003, China

[‡]University of Chinese Academy of Sciences, Beijing 100049, China

Supporting Information



ABSTRACT: A simple colorimetric approach for mercury ion (Hg^{2+}) sensing was developed that was based on the Hg^{2+} -induced deprotection and morphology transition of 1-dodecanethiol ($\text{C}_{12}\text{H}_{25}\text{SH}$)-capped silver nanoprisms (Ag NPRs) upon the presence of iodides at room temperature. The abstraction of $\text{C}_{12}\text{H}_{25}\text{SH}$ from the surface of Ag NPRs by Hg^{2+} led to their deprotection of Ag NPRs and the formation of complexation between silver ions and excess iodide ions. Also, the silver atoms were consumed and moved from the surface of Ag NPRs, accompanying the changes in the particle morphology that resulted in a change of color and UV–vis absorption spectra of the colloidal solution. With increasing concentrations of Hg^{2+} from 10 to 500 nM, the surface plasma resonance spectral band of Ag NPRs emerged as a blue shift and exhibited a good linear relationship, and the limit of detection was 3.3 nM. Furthermore, the developed method was applied for detecting Hg^{2+} in different real water samples with satisfying recoveries over 92%.

KEYWORDS: mercury ions, colorimetric detection, silver nanoprism, morphology transition

INTRODUCTION

Contamination by toxic heavy-metal ions poses a serious threat to human health and the ecological environment. Especially, mercury, which is widely distributed in the air, water, and soil¹ with recognized accumulative character in the environment and biota,^{2–4} can harm the brain, heart, kidneys, lungs, and immune system of people of all ages.⁵ So, we must pay more attention to the determination of mercury. The traditional techniques currently available for the detection of mercury ions (Hg^{2+}) include atomic absorption,⁶ atomic emission,⁷ atomic fluorescence,^{8,9} and inductively coupled plasma mass spectrometry.¹⁰ Although these methods offer excellent sensitivity and multielement analysis, they are sophisticated, costly, complicated processes and time-consuming. Therefore, it is critical to explore a simple, rapid, and inexpensive method for the determination of Hg^{2+} .

Colorimetric methods based on nanomaterials have attracted great attention because of their distinctive advantages such as simplicity and novelty. Recently, a variety of colorimetric methods for Hg^{2+} have been developed by means of

nanomaterials, such as gold nanospheres, gold nanorods combining DNA oligomers,^{11–13} fluorophores,¹⁴ and molecular ligands.^{15,16} Typically, Yang's group developed an approach for visual and fluorescent sensing of Hg^{2+} based on the Hg^{2+} -induced conformational change of a thymine-rich single-stranded DNA and the difference in the electrostatic affinities between single- and double-stranded DNA with gold nanoparticles (Au NPs).¹⁷ Campiglia's group provided a direct way to determine Hg^{2+} with gold nanorods, taking advantage of the strong affinity between gold and mercury.¹⁸ However, these existing methods for sensing Hg^{2+} usually require a rather complicated procedure of the synthesis and modification of Au NPs, and a more facile and economic material as the novel sensor for Hg^{2+} should be developed.

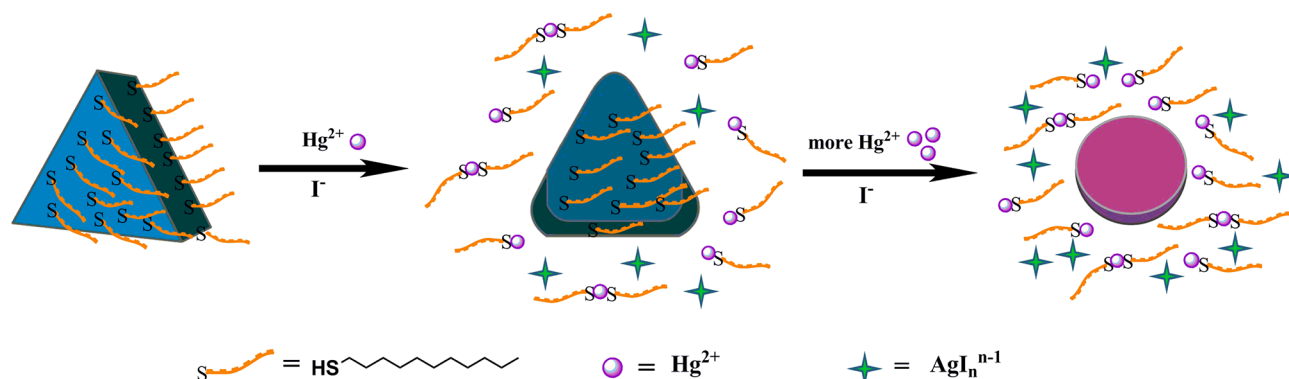
Silver nanoparticles (Ag NPs) exhibit intensive surface plasma resonance (SPR) bands in the wavelength range of 300–900 nm;

Received: September 23, 2012

Accepted: December 13, 2012

Published: December 13, 2012

Scheme 1. Schematic Sensing Mechanism of a Hg^{2+} -Controlled Morphology Transition of 1-Dodecanethiol-Capped Ag NPRs in the Presence of Excess I^-



moreover, they are cost-effective in preparation compared to Au NPs.¹⁹ Ag NPs have now become widely utilized in biological, chemical, and environmental fields because of their simplicity, high sensitivity, and biocompatibility. Some colorimetric sensors have been employed to probe cysteine,²⁰ metal ions,^{21,22} and enzymes²³ based on target-induced aggregation of functionalized Ag NPs, relying on the color change and UV-vis spectral response. Our group has developed a colorimetric method for the detection of trace copper ions (Cu^{2+}) based on the catalytic leaching of silver-coated Au NPs using their sensitive surface properties.²⁴ Two-dimensional arrays and linear chains of Ag NPs were also developed for refractive index sensors.^{25–28} Owing to their higher enhancement factors over other metallic nanoparticles, such as gold and copper, Ag NPs were usually employed as surface enhancement Raman scattering (SERS) substrates of SERS sensors.^{29–31} Our group has also developed an approach to detect arsenic(III) based on the aggregation of glutathione-functionalized Ag NPs using 4-mercaptopyridine as a Raman reporter.³²

As we all know, the common 20–30 nm monodispersed Ag NP solution is bright yellow, while the aggregated Ag NP solution is blue gray, which is not suitable for visual assay. However, anisotropic Ag NPs such as triangular prisms and platelike nanostructures are extensively investigated.³³ These structures are especially interesting because they have plasmonic features in the visible and IR regions. Jiang and Yu presented a method to detect inorganic anions (e.g., Cl^- , Br^- , I^- , H_2PO_4^- , and SCN^-) by using silver nanoplates based on the particle surface electron charging responsible for the shift in the SPR because of the tendency between silver atoms and various inorganic anions.³⁴ Technically, we note that triangular nanoprisms contain three sharp vertices or “tips” that contribute significantly to their optical and electronic properties.^{35,36} When significant rounding occurs, the shapes of the nanomaterials are no longer described as triangular nanoprisms and generally are referred to as nanodisks or, in cases of truncation without rounding, hexagonal nanoprisms,³³ along with a blue shift of the SPR spectra depending on the change in the particle architecture. This fascinating phenomenon would be introduced to build a colorimetric sensor for the determination of heavy-metal ions in aqueous solution. To the best of our knowledge, few literatures were reported on the application of silver nanoprisms (Ag NPRs) in colorimetric sensing detection.

Accordingly, in this study, a simple and cost-effective sensing platform for Hg^{2+} in aqueous solution at room temperature was demonstrated based on 1-dodecanethiol-capped Ag NPRs upon the presence of excess iodide ions (I^-). In the present sensing

system, a colorful Ag NPR colloid was skillfully employed to develop a colorimetric strategy for the detection of Hg^{2+} , based on a Hg^{2+} -controlled morphology transition of Ag NPRs. The results proved that this method had a good performance in terms of selectivity, sensitivity, linearity, and limits of detection for the determination of Hg^{2+} in real water samples.

EXPERIMENTAL SECTION

Reagents. Poly(vinylpyrrolidone) (PVP; $M_w \sim 24000 \text{ g}\cdot\text{mol}^{-1}$), sodium bis(2-ethylhexyl)sulfosuccinate (NaAOT; 99%), and 1-dodecanethiol ($\text{C}_{12}\text{H}_{25}\text{SH}$) were purchased from Aladdin. Silver nitrate (AgNO_3 ; 99%), trisodium citrate ($\text{C}_6\text{H}_5\text{Na}_3\text{O}_7\cdot 2\text{H}_2\text{O}$; 99%), hydrogen peroxide (H_2O_2 ; 30 wt %), sodium borohydride (NaBH_4 ; $\geq 96\%$), potassium bromide (KBr; 99%), potassium iodide (KI; 99%), potassium chloride (KCl; 99%), ethylic acid, sodium acetate, $\text{Hg}(\text{NO}_3)_2$, $\text{Cd}(\text{NO}_3)_2$, MgSO_4 , $\text{Zn}(\text{NO}_3)_2$, $\text{CoCl}_2\cdot 6\text{H}_2\text{O}$, $\text{Pb}(\text{NO}_3)_2$, MnSO_4 , CuSO_4 , FeCl_2 , BaCl_2 , etc., were all received from Sinopharm Chemical Reagent Co., Ltd., China. All of the reagents were of analytical grade and were used without further purification.

Instrumentation. Solutions were prepared with deionized water (18.2 $\text{M}\Omega\cdot\text{cm}$ specific resistance) purified by a Cascada TM LS Ultrapure water system (Pall Corp., USA). The pH measurements were carried out on a PHS-3C meter. Transmission electron microscopy (TEM) analysis was performed on a 10 JEM-1230 electron microscope (JEOL, Ltd., Japan) operating at 100 kV. UV-vis absorption spectra were measured on a Thermo Scientific NanoDrop 2000/2000C spectrophotometer (USA).

Synthesis of Ag NPRs. All glassware used in the following procedure was cleaned in a bath of freshly prepared 3:1 (v/v) HCl/HNO_3 , rinsed thoroughly in water, and dried in air. Double-distilled water was used for all of the experiments. The Ag NPRs were prepared according to a published thermal method³⁷ with slight modifications. Typically, an aqueous solution of AgNO_3 (2.0 mM, 2.5 mL), $\text{C}_6\text{H}_5\text{Na}_3\text{O}_7\cdot 2\text{H}_2\text{O}$ (30 mM, 3 mL), PVP (0.7 mM, 3.0 mL), and H_2O_2 (30 wt %, 120 μL) was mixed in a 100 mL flask and vigorously stirred at 25 $^\circ\text{C}$. NaBH_4 solution (100 mM, 180 μL) was rapidly added to this mixture, generating a colloid that was pale yellow. After 30 min, the colloid darkened to purple/turquoise. The resulting colloids were stored in the dark at room temperature.

Sensing Detection of Hg^{2+} . Rational designed tests were carried out to optimize the sensing conditions. For the sensing detection of Hg^{2+} , aliquots (1.0 mL) of a stock solution containing HAC/NaAc buffer solutions (10 mM, pH 5.0), Ag NPRs (225 μL), NaAOT (0.5 mM), $\text{C}_{12}\text{H}_{25}\text{SH}$ (1.0 μM), and I^- (0.5 mM) were prepared. Then, different concentrations of Hg^{2+} were added to each of the mixture solutions, which were shaken and equilibrated at room temperature for 15 min. Finally, UV-vis absorption spectra were recorded.

Selective Detection of Hg^{2+} . In the experiments of selectivity and practical assay, all samples were tested in a similar manner. We investigated the selectivity of the proposed approach for Hg^{2+} over

other metal ions (Cd^{2+} , Mg^{2+} , Zn^{2+} , Co^{2+} , Pb^{2+} , Mn^{2+} , Cu^{2+} , Fe^{2+} , and Ba^{2+}) under the same optimized conditions.

Analysis of Real Water Samples. Tap water and drinking water samples obtained from our institute and a pond water sample collected from a pond on the campus of Yantai University (Yantai, China) were filtered through a $0.2\ \mu\text{m}$ membrane. The water samples were spiked with standard Hg^{2+} solutions at certain concentrations and then mixed with the stock solutions containing the Ag NPR probe and a HAC/NaAc buffer solution (pH 5.0).

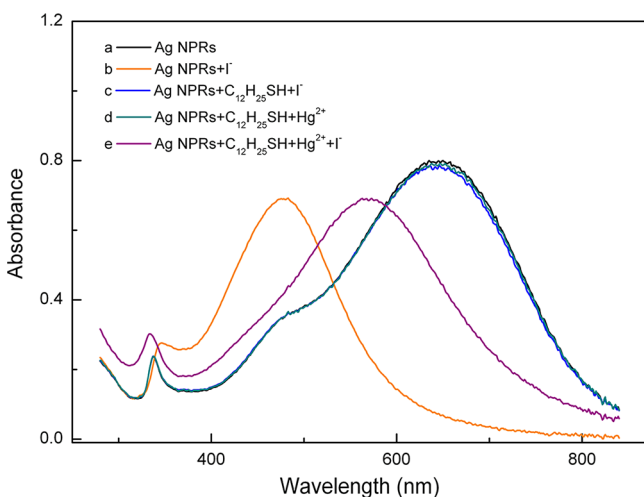


Figure 1. UV-vis spectra of a Ag NPR solution at different conditions: (a) Ag NPRs ($450\ \mu\text{L}$) in a HAC/NaAc buffer; (b) Ag NPRs + I^- ($10\ \mu\text{L}$, $0.1\ \text{M}$); (c) Ag NPRs + $\text{C}_{12}\text{H}_{25}\text{SH}$ ($2\ \mu\text{L}$, $1.0\ \text{mM}$) + I^- ($10\ \mu\text{L}$, $0.1\ \text{M}$); (d) Ag NPRs + $\text{C}_{12}\text{H}_{25}\text{SH}$ ($2\ \mu\text{L}$, $1.0\ \text{mM}$) + Hg^{2+} ($20\ \mu\text{L}$, $0.1\ \text{mM}$); (e) Ag NPRs + $\text{C}_{12}\text{H}_{25}\text{SH}$ ($2\ \mu\text{L}$, $1.0\ \text{mM}$) + Hg^{2+} ($20\ \mu\text{L}$, $0.1\ \text{mM}$) + I^- ($10\ \mu\text{L}$, $0.1\ \text{M}$).

RESULTS AND DISCUSSION

Proposed Mechanism for the Sensing System. Scheme 1 outlined the proposed sensing mechanism. Initially, the Ag NPRs were capped by 1-dodecanethiol because of the strong affinity of the thiol head groups on the silver surfaces. Thus, I^- could not be attached to the surface of the Ag NPRs, and the shapes of the Ag NPRs were frozen. As indicated in Figure 1 (curves a–c), I^- induced obvious absorption changes of Ag NPRs because of the formation of a strong Ag–I bond.^{34,38} However, this change could be blocked by the surface modification of 1-dodecanethiol relying on the thiol-frozen action to the surface of Ag NPRs.³⁹ The thiol group ($-\text{SH}$) adsorbed more strongly than I^- because of $-\text{SH}$ donating a higher electron density into the Ag NPs.³⁴ Herein, 1-dodecanethiol was employed as a protective agent to prevent silver surface reaction from I^- .

However, in the presence of Hg^{2+} , Hg^{2+} could first abstract thiols from the active “tips” area of the Ag NPRs because of the higher binding energy of thiols on silver atomic planes in (111) compared with other planes such as (110) and (100).³⁹ As a result, the silver atoms in the “tips” area of the Ag NPRs got free and were consumed by I^- . As shown in Figure 1 (curves d and e), a satisfying absorption spectrum was obtained (curve e), while no obvious change was observed with Hg^{2+} only (curve d). It is undoubted that the abstraction of thiols by Hg^{2+} was associated with the fact that the stability constant ($\log K_f$) of $\text{Hg}(\text{SCN})_n$ (ca. 21.8) is larger than that of $\text{Ag}(\text{SCN})_n$ (ca. 10.08).⁴⁰ $-\text{SCN}$ is similar to $-\text{SH}$, which can bind strongly onto the surfaces of Ag NPs, so Hg^{2+} are capable of removing thiolates chemisorbed on the surface of the Ag NPRs, thus allowing excess I^- to invade the bare surface of the Ag NPRs, which could result in the absorption changes.

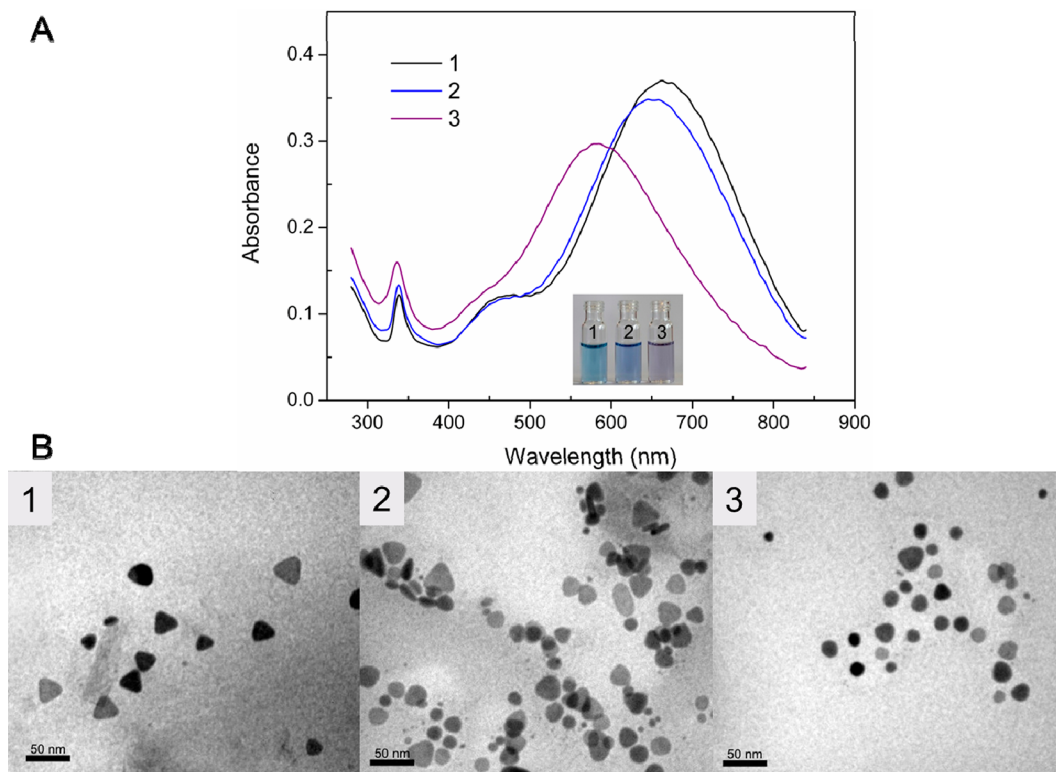


Figure 2. (A) UV-vis spectra (the inset image corresponds to the colorimetric response) and (B) TEM images of the Ag NPRs in the absence (1) and presence of $0.7\ \mu\text{M}$ (2) and $1.5\ \mu\text{M}$ (3) Hg^{2+} . The incubation time was 15 min.

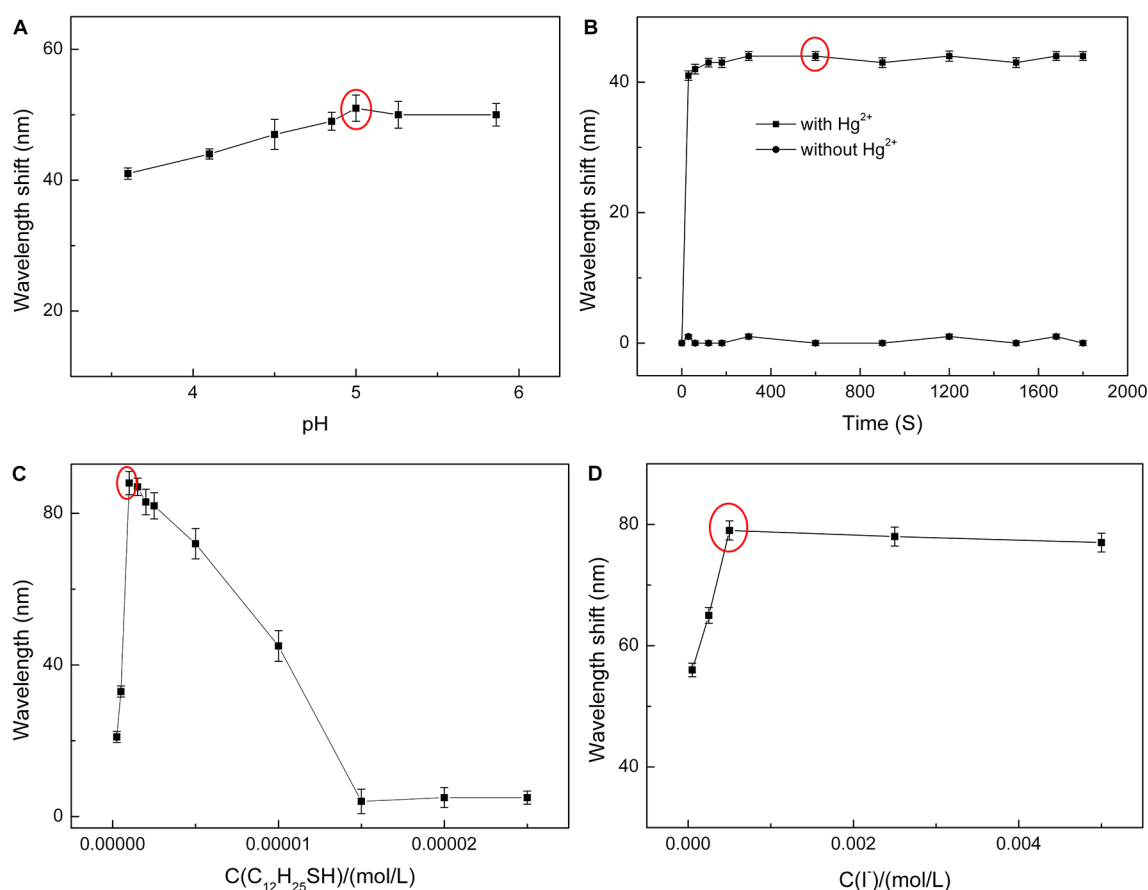


Figure 3. (A) Effect of the pH value of a HAc/NaAc buffer solution on the wavelength shift of the $I^-/1$ -dodecanethiol-capped Ag NPR system in the presence of $1.0 \mu M Hg^{2+}$. (B) Plot of the wavelength shift of the Ag NPRs versus the reaction time in the presence of Hg^{2+} . (C) Effect of the concentration of 1-dodecanethiol on the wavelength shift of Ag NPRs. (D) Effect of the concentration of iodides in the sensing system. The error bars represent the standard deviations based on three independent measurements.

As expected, when Hg^{2+} were introduced to the solution, a blue shift of the in-plane dipole surface plasmon band occurred (Figure 2A), and the color of silver colloids changed accordingly from blue to purple (inset photograph of Figure 2A). These significant changes were further evidenced by TEM images, which revealed the original triangular shapes (Figure 2B-1) in the absence of Hg^{2+} , passivation triangle shapes (Figure 2B-2, with $700 nM Hg^{2+}$), and even circular shapes (Figure 2B-3, with $1500 nM Hg^{2+}$) in the presence of Hg^{2+} . Interestingly, with increasing of Hg^{2+} , further rounding of the “tips” of the Ag NPRs occurred gradually as a function of I^- . The morphology transition of Ag NPRs from triangle to disk occurred as the silver atoms were consumed by minute dissolved oxygen, and the formation of AgI_n^{n-1} complexes relied on their strong interaction tendency.^{38,41} The shape distributions of the Ag NPs upon the addition of different concentrations of Hg^{2+} were also analyzed considering the inhomogeneity of particles. The results indicated that the morphology transition occurred gradually from triangle to disk with an increase of Hg^{2+} (see Figure S1 in the Supporting Information). In addition, a series of better TEM images were added to show the fascinating changes (see Figure S2 in the Supporting Information). Namely, more and more thiols were abstracted from the surface of the Ag NPRs by Hg^{2+} , allowing the bare surface silver atoms to be consumed by excess electron-rich I^- under an acidic medium in air, and subsequently the shapes of the Ag NPRs changed. Therefore, a colorimetric method for sensing Hg^{2+} was presented based on the morphology transition of 1-

dodecanethiol-capped Ag NPRs in the presence of excess I^- in aqueous solution at room temperature by a blue shift of the SPR.

Optimization of the Responsive Conditions of the Sensing System. For the best performance of our proposed sensing system, the optimized conditions were investigated. A wavelength shift of the in-plane dipole surface plasmon band of the Ag NPRs was employed to determine the conditions, including the pH, addition time, and optimum concentration of 1-dodecanethiol and iodides in this system.

The effect of the pH on the proposed system was tested in the presence of $1.0 \mu M Hg^{2+}$. As shown in Figure 3A, the sensing system was insensitive to the pH in the range of 3.6–5.9. The positively charged H^+ can accelerate the displacement reaction of Hg^{2+} , with the thiols chemisorbed on the surfaces of the Ag NPRs; that is to say, Ag–S bonds were easily broken by Hg^{2+} in the partial acidic conditions.^{40,42} However, pH toward lower values was not in favor of erosion to the surface of the Ag NPRs by I^- .³⁴ However, at pH 5.0, the morphology transition of Ag NPRs occurred to the greatest extent relatively. So, we employed pH at 5.0 in favor of abstraction of thiols on the surface of the Ag NPRs by Hg^{2+} . The reaction time was also studied under the optimized pH in the presence of Hg^{2+} . It is noteworthy that the sensing system achieved a balance at 15 min, as shown in Figure 3B; there was a maximum wavelength shift at 15 min that remained almost constant for 15–30 min. Therefore, 15 min was chosen as the time of recording absorption spectra in this work.

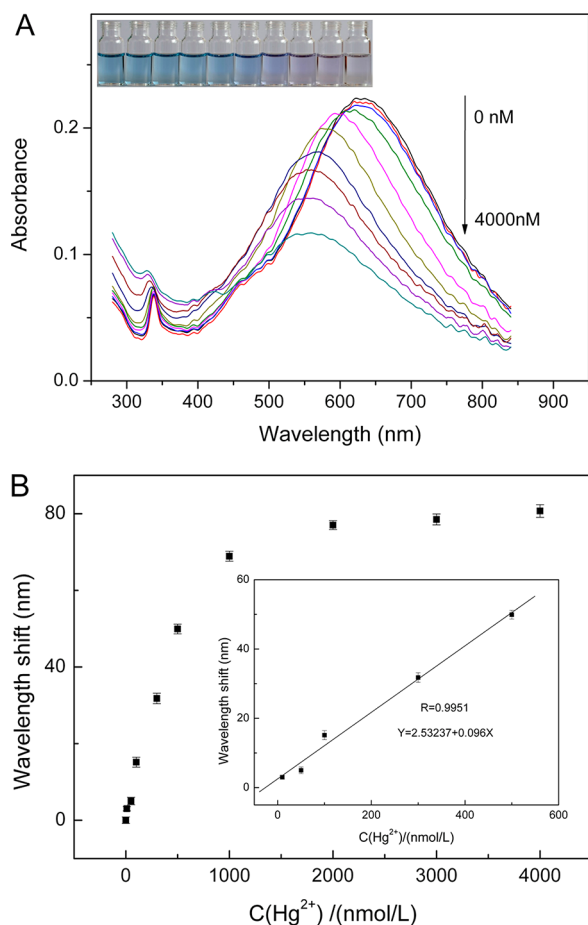


Figure 4. (A) UV-vis absorption spectra of the Ag NPRs after the addition of different concentrations of Hg^{2+} . The inset image is the colorimetric response to different concentrations of Hg^{2+} . (B) Wavelength shift of the Ag NPRs with different concentrations of Hg^{2+} (10–4000 nM). The inset shows a plot of the wavelength shift versus the different concentrations of Hg^{2+} (10–500 nM). The incubation time was 15 min, and the pH value of the solutions was 5.0. The error bars represent the standard deviations based on three independent measurements.

A study focusing on the effect of the different concentrations of 1-dodecanethiol was also provided. The 1-dodecanethiol molecules played an important role as protective agents³⁹ of the Ag NPRs, which ensured good selectivity in this system. Thiols were combined with the silver surface through Ag–S bonds, which could hinder I^- adsorption onto the silver prism surface in the absence of Hg^{2+} . Namely, upon the addition of Hg^{2+} , thiols were abstracted from the surface, allowing I^- to erode the Ag NPRs. When the concentration of the thiols was high, Hg^{2+} tended to combine to free thiols, and this resulted in a lower wavelength shift, which would reduce the sensitivity of our proposed sensing system. So, a certain concentration of 1.0 μM was employed in the solution, as marked in Figure 3C. Besides, we also investigated the effect of the concentrations of iodides on the sensing system. As an invading agent, I^- could induce the Ag NPR morphology transition by complexing with bare silver atoms on the surface in air. With increasing concentrations of I^- , the wavelength shift, depending on the change in the particle architecture, increased gradually and went to a balance. Finally, the concentration of 0.5 mM was selected in the system, as seen from Figure 3D.

Sensitivity and Selectivity for Sensing Hg^{2+} . To evaluate the sensitivity of the sensor, the UV-vis spectra of

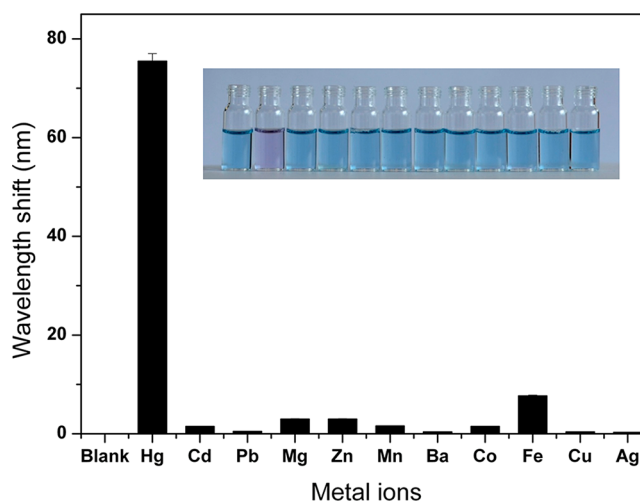


Figure 5. Wavelength shift of the Ag NPR solution in the presence of 2 μM Hg^{2+} and 100-fold other metal ions, respectively, including Cd^{2+} , Pb^{2+} , Mg^{2+} , Zn^{2+} , Mn^{2+} , Ba^{2+} , Co^{2+} , Fe^{2+} , Cu^{2+} , and Ag^+ . The inset shows corresponding color photographic images. The incubation time was 15 min. The error bars represent the standard deviations based on three independent measurements.

Table 1. Recoveries for the Determination of Hg^{2+} in Real Water Samples ($n = 3$)

sample	added (μM)	found (μM)	recovery (%)	RSD (%)
tap water	0	nd ^a		
	0.200	0.195	97.5	0.69
	0.400	0.417	104.2	1.68
drinking water	0	nd ^a		
	0.200	0.185	92.5	1.03
	0.400	0.415	103.8	1.25
lake water	0	nd ^a		
	0.200	0.213	106.5	1.08
	0.400	0.434	108.5	0.86

^and means not detected.

the Ag NPR solutions in different concentrations of Hg^{2+} were recorded. Under optimized conditions, different concentrations of Hg^{2+} were added to the solution and incubated for 15 min. As shown in Figure 4A, upon the addition of increasing concentrations of Hg^{2+} , the SPR band emerged as a blue shift, which was attributed to the morphology transition of Ag NPRs in the state of excess iodides. Therefore, the wavelength shift of the in-plane dipole surface plasmon band of Ag NPRs was employed in the quantitative analysis of Hg^{2+} . A typical plot of the wavelength shift versus Hg^{2+} concentrations (10–4000 nM) is shown in the inset of Figure 4B, and a satisfying linear relationship, $\Delta\lambda = 2.53237 + 0.096c$ (nm), was obtained over the range of 10–500 nM with the correlation coefficient of 0.995 (here, $\Delta\lambda$ means the wavelength shift). The results suggest that this probe can be used to detect Hg^{2+} with a detection limit of 3.3 nM calculated by a signal-to-noise ratio of 3 ($3\sigma/S$). Here, S means the slope of the linear equation and σ means the standard deviation of blank measurements. Thus, the detection limit $\text{DL} = 3(0.10562/0.096) = 3.3$ nM.

To realize the selectivity of this probe toward Hg^{2+} , the competitive metal ions, including Cd^{2+} , Pb^{2+} , Mg^{2+} , Zn^{2+} , Mn^{2+} , Ba^{2+} , Co^{2+} , Fe^{2+} , Cu^{2+} , and Ag^+ , were examined under optimized conditions. The wavelength shift and corresponding photographic images of the Ag NPRs containing 2 μM Hg^{2+}

and 100-fold other ions, respectively, are vividly shown in Figure 5. The results demonstrated that only Hg^{2+} could cause the significant morphology transition of Ag NPRs, and the 100-fold excess other metal ions had no evident effect on the SPR band and the color of the colloid under optimized conditions. The above results indicated that our proposed method exhibits high selectivity toward Hg^{2+} ions because of the strong affinity between Hg^{2+} and the thiol groups.

Practical Application. To further evaluate the potential application of this sensing system in some real samples, the sensor was tentatively applied to sensing Hg^{2+} in real samples such as tap water, drinking water, and pond water samples. Comfortingly, satisfactory recoveries of Hg^{2+} were obtained in three different real samples, with recoveries of over 92%, as shown in Table 1. Importantly, the results presented in Table 1 also demonstrated that the compositions of real samples did not significantly interfere with the detection of Hg^{2+} , indicating the potential applications of our proposed colorimetric method for the analysis of Hg^{2+} in complicated environmental samples.

CONCLUSIONS

A new and rapid colorimetric sensing method for the detection of Hg^{2+} was developed based on the morphology transition of Ag NPRs at room temperature. It offered many advantages such as simplicity, rapidity, high sensitivity, and excellent selectivity for the response to mercury in aqueous media. The materials used in this assay were inexpensive and available commercially. Compared with other reports for the detection of Hg^{2+} , our method provided a good performance as well (see Table S1 in the Supporting Information). Constructively, we successfully employed the brightly colorful silver colloid to develop a new colorimetric method for Hg^{2+} , which will enrich the applications of Ag NPs in the colorimetric sensing detection of heavy-metal ions. Furthermore, this sensing system exhibits satisfying performances in real environmental water samples, which indicates a promising potential for application in environmental area. In view of this development, we will develop other colorimetric sensing probes by using economic Ag NPRs.

ASSOCIATED CONTENT

Supporting Information

Shape distributions of a Ag NPR sensing system before and after the addition of different concentrations of Hg^{2+} , additional TEM images of Ag NPRs before and after the addition of different concentrations of Hg^{2+} , and a table of comparison of other methods for the detection of Hg^{2+} with our proposed method. This material is available free of charge via the Internet at <http://pubs.acs.org>.

AUTHOR INFORMATION

Corresponding Author

*E-mail: lxchen@yic.ac.cn.

Notes

The authors declare no competing financial interest.

ACKNOWLEDGMENTS

This work was financially supported by the Scientific Research Foundation for the Returned Overseas Chinese Scholars, State Education Ministry, the National Natural Science Foundation of China (Grant 21275158), the Innovation Projects of the Chinese Academy of Sciences (Grant KZCX2-EW-206), and the 100 Talents Program of the Chinese Academy of Sciences.

REFERENCES

- (1) Miller, J. R.; Rowland, J.; Lechler, P. J.; Desilets, M.; Hsu, L. C. *Water, Air, Soil Pollut.* **1996**, *86*, 373–388.
- (2) Eisler, R. *Environ. Geochem. Health* **2003**, *25*, 325–345.
- (3) Wang, Q. R.; Kim, D.; Dionysiou, D. D.; Sorial, G. A.; Timberlake, D. *Environ. Pollut.* **2004**, *131*, 323–336.
- (4) Tchounwou, P. B.; Ayensu, W. K.; Ninashvili, N.; Sutton, D. *Environ. Toxicol.* **2003**, *18*, 149–175.
- (5) Report to congress, Potential Export of Mercury Compounds from the United States for Conversion to Elemental Mercury, Oct 14, 2009.
- (6) Kopysc, E.; Pyrzynska, K.; Garbos, S.; Bulska, E. *Anal. Sci.* **2000**, *16*, 1309–1312.
- (7) Gomez-Ariza, J.; Lorenzo, F.; Garcia-Barrera, T. *Anal. Bioanal. Chem.* **2005**, *382* (382), 485–492.
- (8) Yu, L.; Yan, X. *At. Spectrom.* **2004**, *25*, 145–153.
- (9) Bloxham, M. J.; Hill, S. J.; Worsfold, P. J. *J. Anal. At. Spectrom.* **1996**, *11*, 511–514.
- (10) Li, Y.; Chen, C.; Li, B.; Sun, J.; Wang, J.; Gao, Y.; Zhao, Y.; Chai, Z. *J. Anal. At. Spectrom.* **2006**, *21*, 94–96.
- (11) Lee, J. S.; Han, Min., S.; Mirkin, C. A. *Angew. Chem., Int. Ed.* **2007**, *46*, 4093–4096.
- (12) Liu, C. W.; Hsieh, Y. T.; Huang, C. C.; Lin, Z. H.; Chang, H. T. *Chem. Commun.* **2008**, 2242–2244.
- (13) Lee, J. S.; Mirkin, C. A. *Anal. Chem.* **2008**, *80*, 6805–6808.
- (14) Ye, B. C.; Yin, B. C. *Angew. Chem., Int. Ed.* **2008**, *47*, 8386–8389.
- (15) Huang, C. C.; Chang, H. T. *Chem. Commun.* **2007**, 1215–1217.
- (16) Chen, L.; Lou, T. T.; Yu, C. W.; Kang, Q.; Chen, L. X. *Analyst* **2011**, *136*, 4770–4773.
- (17) Wang, H.; Wang, Y. X.; Jin, J. Y.; Yang, R. H. *Anal. Chem.* **2008**, *80*, 9021–9028.
- (18) Rew, M.; Hernandez, F. E.; Campiglia, A. D. *Anal. Chem.* **2006**, *78* (2), 445–451.
- (19) Kelly, K. L.; Coronado, E.; Zhao, L. L.; Schatz, G. C. *J. Phys. Chem. B* **2003**, *107*, 668–677.
- (20) Zhang, M.; Ye, B. C. *Anal. Chem.* **2011**, *83*, 1504–1509.
- (21) Yoosaf, K.; Ipe, B. I.; Suresh, C. H.; Thomas, K. G. *J. Phys. Chem. C* **2007**, *111*, 12839–12847.
- (22) Ma, Y. R.; Niu, H. Y.; Zhang, X. L.; Cai, Y. Q. *Chem. Commun.* **2011**, *47*, 12643–12645.
- (23) Wei, H.; Chen, C. G.; Han, B. Y.; Wang, E. K. *Anal. Chem.* **2008**, *80*, 7051–7055.
- (24) Lou, T. T.; Chen, L. X.; Chen, Z. P.; Wang, Y. Q.; Chen, L.; Li, J. H. *ACS Appl. Mater. Interfaces* **2011**, *3*, 4215–4220.
- (25) Kinnan, M. K.; Kachan, S.; Simmons, C. K.; Chumanov, G. J. *Phys. Chem. C* **2009**, *113*, 7079–7084.
- (26) Malinsky, M. D.; Kelly, K. L.; Schatz, G. C.; Van Duyne, R. P. *J. Am. Chem. Soc.* **2001**, *123*, 1471–1482.
- (27) Haes, A. J.; Chang, L.; Klein, W. L.; Van Duyne, R. P. *J. Am. Chem. Soc.* **2005**, *127*, 2264–2271.
- (28) Miller, M. M.; Lazarides, A. A. *J. Phys. Chem. B* **2005**, *109*, 21556–21565.
- (29) Tao, A.; Kim, F.; Hess, C.; Goldberger, J.; He, R.; Sun, Y.; Xia, Y.; Yang, P. D. *Nano Lett.* **2003**, *3*, 1229–1233.
- (30) Shanmukh, S.; Jones, L.; Driskell, J.; Zhao, Y.-P.; Dluhy, R.; Tripp, R. A. *Nano Lett.* **2006**, *6*, 2630–2636.
- (31) Lucotti, A.; Giuseppe, Z. *Sens. Actuators, B* **2007**, *121*, 356–364.
- (32) Li, J. L.; Chen, L. X.; Lou, T. T.; Wang, Y. Q. *ACS Appl. Mater. Interfaces* **2011**, *3* (10), 3936–3941.
- (33) Millstone, J. E.; Hurst, S. J.; Métraux, G. S.; Cutler, J. I.; Mirkin, C. A. *Small* **2009**, *5* (6), 646–664.
- (34) Jiang, X. C.; Yu, A. B. *Langmuir* **2008**, *24* (8), 4300–4309.
- (35) Kelly, K. L.; Coronado, E.; Zhao, L. L.; Schatz, G. C. *J. Phys. Chem. B* **2003**, *107* (3), 668–677.
- (36) Shuford, K. L.; Ratner, M. A.; Schatz, G. C. *J. Chem. Phys.* **2005**, *123*, 114713–721.
- (37) Métraux, G. S.; Mirkin, C. A. *Adv. Mater.* **2005**, *17* (4), 412–415.

- (38) Linnert, T.; Mulvaney, P.; Henglein, A. *J. Phys. Chem.* **1993**, *97*, 679–682.
- (39) Jiang, X. C.; Zeng, Q. H.; Yu, A. B. *Langmuir* **2007**, *23*, 2218–2223.
- (40) Liu, D. B.; Qu, W. S.; Chen, W. W.; Zhang, W.; Wang, Z.; Jiang, X. Y. *Anal. Chem.* **2010**, *82* (23), 9606–9610.
- (41) Henglein, A. *Chem. Mater.* **1998**, *10*, 444–450.
- (42) Zhang, F. Q.; Zeng, L. Y.; Yang, C.; Xin, J. W.; Wang, H. Y.; Wu, A. G. *Analyst* **2011**, *136*, 2825–2830.